

## Deformation of grafted polymer layers in strong shear flows

J. L. Harden<sup>1,2</sup> and M. E. Cates<sup>2</sup>

<sup>1</sup>*Cavendish Laboratory, Cambridge University, Madingley Road, Cambridge CB3 0HE, United Kingdom*

<sup>2</sup>*Department of Physics and Astronomy, University of Edinburgh, James Clerk Maxwell Building, King's Buildings, Mayfield Road, Edinburgh EH9 3JZ, United Kingdom*

(Received 30 June 1995)

We present a theoretical approach for studying the deformation of grafted polymer layers in strong shear flows that calculates the deformation of grafted chains and the solvent flow profile within the layer in a mutually consistent fashion. We illustrate this approach by considering the deformation of Alexander–de Gennes brushes in simple shear flows. Our model predicts nonuniform deformation of grafted polymer chains and appreciable swelling of brushes for shear rates exceeding  $\tau^{-1} \simeq k_B T / (\eta \xi_0^3)$ , the characteristic hydrodynamic relaxation rate of a blob of the unperturbed brush. An asymptotic swelling of  $\sim 25\%$  for  $\dot{\gamma} \tau \gg 1$  is predicted, in accordance with theories of brush response to strong applied tangential boundary forces. We briefly compare our results to recent experiments and to theories of brush deformation in shear conditions and outline the generalization of our approach to more realistic models of grafted polymer layers and to adsorbed polymer layers in strong flows.

PACS number(s): 36.20.Ey, 68.10.Et, 83.50.Lh

### I. INTRODUCTION

The properties of polymer brushes have been studied intensively during the past two decades. The equilibrium properties of polymer brushes are now well understood and are reviewed in Refs. [1,2]. Recent studies have focused on the properties of polymer brushes subjected to shear and/or compressional forces [3–14]. Such forces may occur when brushes in solution are exposed to solvent flows or when two brush-bearing surfaces in contact are forced into relative motion.

In the case of polymer brushes subjected to solvent flows, there is evidence that the brush thickness can increase in sufficiently high shear-rate flows [3,5]. These experiments utilized a modified surface forces apparatus to study the normal forces between brush-bearing surfaces initially separated by a solvent gap and put into relative lateral motion. Above a critical value of relative velocity, an abrupt increase in the normal force was observed. This behavior was interpreted in terms of the closing of the solvent gap due to brush swelling under shear. For the parameters studied, brush swelling of  $\sim 20\%$  was inferred. Recently, neutron reflectivity experiments have been developed for *in situ* studies of grafted polymer conformation in controlled shear flows [7–9]. These experiments provide motivation for theoretical modeling of grafted polymer layers in strong flows.

To date, theoretical studies have taken two directions. In the linear regime, appropriate for weak flows, studies based on the Brinkman equation for flow through porous media have been used to calculate solvent velocity profiles for various models of equilibrium brushes [10,11]. Implicit in these studies is the assumption that solvent flow does not appreciably perturb the brush structure. For the Alexander–de Gennes model of the poly-

mer brush [15,16], the density is uniform throughout the brush and solvent flow profiles are predicted to decay exponentially into the brush with a characteristic penetration depth  $l_p \simeq \xi_0$ , the mean distance between grafting points [10]. Self-consistent mean-field models predict a more diffuse brush structure, with a monomer density profile that vanishes quadratically at the free surface of the brush [17,18]. In this case, weak solvent flows are predicted to penetrate much deeper into the brush [11].

In the nonlinear regime, appropriate for strong flows, several models have been proposed for the deformation of brushes [12–14]. These studies effectively ignore the details of solvent flow inside a brush by modeling the solvent-brush frictional forces by an *ad hoc* shear force  $f_{\parallel}$  applied to the free surface of a brush. This necessarily leads to uniform stretching of the grafted chains. For asymptotically large  $f_{\parallel}$ , moderate brush swelling of 25% [13] to 33% [14] is predicted, values consistent with experiment [3]. However, a quantitative comparison with experiment is difficult since the shear rate  $\dot{\gamma}$  is the relevant experimental control parameter, whereas the effective boundary shear force  $f_{\parallel}$  is unknown. In order to make more direct contact with experiments, a more complete theory is necessary. In this paper, we report a theoretical attempt to determine, in a mutually consistent fashion, both brush deformation and solvent penetration into a brush in the strong deformation regime. Our approach represents a starting point towards a realistic theory of grafted and adsorbed polymer layers in strong shear flows.

### II. MODEL

Our model for brush deformation in solvent flows is a scaling theory based on a modification of the model of

Refs. [12,13] to account for the nonuniform stretching of grafted polymer chains in flows [19–22]. We have recently applied this type of model to study the deformation of polymer brushes on porous grafting surfaces subject to permeation flows through the grafting surface [23].

We consider a monodisperse brush of polymers with degree of polymerization  $N$  grafted to a planar surface at grafting density  $\sigma = \xi_0^{-2}$  and exposed to an external linear shear flow of solvent with shear rate  $\dot{\gamma}$ . We restrict our attention to high grafting densities  $\xi_0 \ll R_F \simeq N^{3/5}a$  and for the purposes of illustrating our approach adopt the Alexander–de Gennes ansatz that all chains in the brush behave alike. Thus we represent the chains in the brush as strings of excluded-volume blobs, assume that all chain ends are at the outer edge of the brush, and write the free energy per chain as a sum of an elastic term  $F_{el}$  involving the conformation of a deformed Gaussian string of blobs and an osmotic term  $F_{int}$  involving interactions between blobs. Note that we do *not* assume a uniform stretching of the chains as considered previously [12–14]. Instead, the internal structure of the layer and the velocity profile are determined in a mutually consistent manner. Of course, in a truly self-consistent approach the Alexander–de Gennes ansatz would have to be relaxed. Although this lies beyond the scope of the present work, we will present elsewhere the results of an approach in which this assumption is partially relaxed [24].

In the absence of flow, the Alexander–de Gennes description results in a brush of thickness  $H \sim N\xi_0^{-2/3}$  formed of close-packed blobs of size  $\xi_0$  [15,16]. In the presence of strong shear flow, however, the grafted chains stretch and tilt away from the normal direction, leading to a somewhat distorted brush within which there is some (unknown) solvent flow profile  $\vec{V} = V(z)\vec{x}$ . We picture this deformed brush as consisting of tilted chains of blobs [19], as sketched in Fig. 1. Since the chain extension is due to the integrated hydrodynamic drag on each chain rather than a force applied to the chain ends, the hydrodynamic blob size  $\xi$  and chain tilt angle  $\theta$  are not constants, but are functions of the distance from the

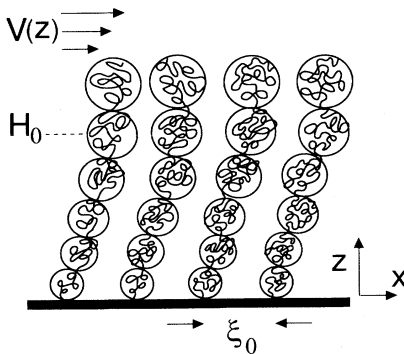


FIG. 1. Sketch of an extended brush in a strong solvent shear flow  $\vec{V}(z) \sim \dot{\gamma}z\vec{x}$ , with  $\xi(z) < \xi_0$  and  $H > H_0$ , where  $\xi_0$  and  $H_0$  are the equilibrium blob size and brush thickness in the absence of flow.

grafting plane, which we must determine self-consistently with the solvent flow profile in the brush. (Note that this is an intrinsically nonlinear problem.)

The elastic energy per chain is obtained by considering each chain as a stretched Gaussian string of blobs and may generally be written [17,23] as

$$F_{el} = \tilde{c}_1 k_B T \int_0^L \frac{ds}{\xi(s)}, \quad (1)$$

where  $a$  is the monomer size,  $s$  is an arc-length coordinate,  $L$  is the total arc length of a tilted chain of blobs, and  $\tilde{c}_1$  is a dimensionless constant of order unity.

Consider now a slab of thickness  $\xi(s)$  at some height  $z(s)$  from the grafting surface. Since the chains are stretched such that  $\xi < \xi_0$ , the volume fraction of blobs in this slab is below the semidilute threshold and hence the local interaction between chains may be approximated by a virial expansion in the blob density [12,13]. The local interaction energy per blob is of order  $k_B T [\xi^2(s)/\xi_0^2 \cos \theta(s)]$ , where  $\theta(s)$  is the local tilt angle measured from the  $\vec{z}$  direction and hence the interaction energy per chain has the form

$$\begin{aligned} F_{int} &= \tilde{c}_2 k_B T \int_0^L \frac{ds}{\xi(s)} \frac{\xi(s)^2}{\xi_0^2 \cos \theta(s)} \\ &= \tilde{c}_2 \frac{k_B T}{\xi_0^2} \int_0^L ds \frac{\xi(s)}{\cos \theta(s)}, \end{aligned} \quad (2)$$

where  $\tilde{c}_2$  is another dimensionless constant of order unity. Our estimate of the free energy per deformed chain is given by the sum of the contributions from Eqs. (1) and (2). Using these, one can define an effective chain tension  $\tilde{t}(s)$  as follows. Consider a short section of chain of length  $\Delta s$  containing  $\Delta n$  monomers. Equations (1) and (2) give the free energy of this section of chain as  $\Delta F = k_B T [\tilde{c}_1 \xi(s)^{-1} + \tilde{c}_2 \xi_0^{-2} \xi(s) / \cos \theta(s)] \Delta s$ . This expression may be written exclusively in terms of  $\Delta x$ ,  $\Delta z$ , and  $\Delta n$  by using  $\Delta s^2 = \Delta x^2 + \Delta z^2$ ,  $\cos \theta = \Delta z / \Delta s$ , and the local expression for chain stretching under external tension,  $\Delta s \simeq \xi^{-2/3} a^{5/3} \Delta n$  [19,23], to eliminate  $\xi$  and  $\theta$  from  $\Delta F$ . Subsequent variation of  $\Delta F$  with respect to  $\Delta x$  at fixed  $\Delta n$  and  $\Delta z$  and of  $\Delta F$  with respect to  $\Delta z$  at fixed  $\Delta n$  and  $\Delta x$  give the components  $t_x$  and  $t_z$  of the effective local chain tension as

$$\frac{t_x(s)}{k_B T} = c_1 \frac{\sin \theta(s)}{\xi(s)} + c_2 \frac{\xi(s)}{\xi_0^2} \tan \theta(s), \quad (3)$$

$$\frac{t_z(s)}{k_B T} = c_1 \frac{\cos \theta(s)}{\xi(s)} - c_2 \frac{\xi(s)}{\xi_0^2} \left( \frac{2 - \cos^2 \theta(s)}{\cos^2 \theta(s)} \right), \quad (4)$$

where  $c_1 = 5\tilde{c}_1/2$  and  $c_2 = \tilde{c}_2/2$ . This effective tension determines the local departure from equilibrium of a representative chain, under conditions where all chains are constrained to behave identically. It already contains osmotic terms and so should not be confused with the (purely elastic) chain tension in a deformed Gaussian chain, which, within a nonscaling, mean-field approach to brushes [17,18], is balanced by osmotic pressure gra-

dients. Our effective tension is constructed so that, in the absence of flow, the equilibrium condition is for  $\vec{t}$  to vanish ( $t_x = t_z = 0$ ). Indeed, if one demands that both  $\xi = \xi_0$  and  $\theta = 0$  in the absence of flow (as in the equilibrium Alexander-de Gennes brush), this fixes the constants as  $c_1 = c_2 = 1$ . We use this fact below.

In mechanical equilibrium, the hydrodynamic drag on a short section of chain of length  $\Delta s$  at  $z(s)$  must be balanced by the differential tension on this section of chain. Assuming laminar flow with  $\vec{V} = V(z)\vec{x}$  in the brush, this implies  $t_z = 0$  and  $\Delta t_x = [\partial t_x(s)/\partial s]\Delta s = c_3\eta V(s)\Delta s$ , where  $c_3$  is another dimensionless constant discussed below. [ $c_3\eta V(s)\Delta s$  represents the drag force on a linear string of Stokes blobs of length  $\Delta s$ .] These requirements lead to

$$\xi(z) = \alpha \frac{\cos^{3/2} \theta(z)}{[2 - \cos^2 \theta(z)]^{1/2}} \xi_0, \quad (5)$$

$$\begin{aligned} \frac{t_x(z)}{k_B T} &= c_1 \frac{\sin \theta(z)}{\xi(z)} + c_2 \frac{\xi(z)}{\xi_0^2} \tan \theta(z) \\ &= c_3 \frac{\eta}{k_B T} \int_z^H dz' \frac{V(z')}{\cos \theta(z')}, \end{aligned} \quad (6)$$

where  $\alpha = (c_2/c_1)^{1/2}$ ,  $H$  is the thickness of the deformed brush, and we have changed the independent variable to  $z$ , the normal distance from the grafting surface.

The shear stress  $\sigma_{xz}$  in the brush is the sum of the contributions from the viscous dissipation due to solvent flow  $\sigma_{xz}^{(s)} = \eta dV/dz$  and from the elastic deformation of polymer chains  $\sigma_{xz}^{(p)}$ . The polymer contribution  $\sigma_{xz}^{(p)}$  may be viewed as the product of the effective lateral chain tension  $t_x(z)$  and the number density of chains crossing the plane at height  $z$ :  $\sigma_{xz}^{(p)} = t_x(z)/\xi_0^2$ . Requiring that the total shear stress is uniform throughout the grafted layer,  $d\sigma_{xz}/dz = 0$ , gives an additional relation between chain conformation and solvent velocity in the brush

$$\frac{d^2 V}{dz^2} = c_3 \frac{1}{\xi_0^2} \frac{V(z)}{\cos \theta(z)}. \quad (7)$$

Note that although Eq. (7) resembles a Brinkman equation, its origin and interpretation are quite different since it arises explicitly from chain tension effects.

Equations (5)–(7) are subject to appropriate boundary conditions at  $z = 0$  and  $z = H$ . We assume no-slip boundary conditions at the grafting surface and continuity of shear stress at the free surface of the brush. Furthermore, we assume that the effective tension Eq. (6) vanishes at the free end of each chain. Thus our boundary conditions are  $V = 0$  at  $z = 0$ , and  $dV/dz = \dot{\gamma}$  and  $\theta = 0$  at  $z = H$ .

For a given brush thickness  $H$ , Eqs. (5)–(7) together with the above boundary conditions uniquely determine  $V(z)$ ,  $\xi(z)$ , and  $\theta(z)$  as a function of the solvent shear rate outside the brush  $\dot{\gamma}$  and the equilibrium brush parameters  $N$  and  $\xi_0$ . The appropriate brush thickness is then obtained by demanding that a chain of blobs stretched to height  $H$  has  $N$  monomers via the conservation relation

$$N = c_4 \int_0^H \frac{dz}{\xi(z) \cos \theta(z)} \left( \frac{\xi(z)}{a} \right)^{5/3}, \quad (8)$$

where  $c_4$  is another constant of order unity.

The solution of our model equations requires a numerical approach. To facilitate this analysis, we choose for definiteness to set the unknown numerical constants  $c_3$  and  $c_4$ , along with  $c_1$  and  $c_2$ , to unity and reformulate these equations as follows. Using Eq. (5), we eliminate  $\xi(z)$  from Eq. (6) and then differentiate both sides with respect to  $z$ . The resulting differential equation, along with Eqs. (7) and (8), is then put into dimensionless form using the scaled variables  $\zeta = z/\xi_0$  and  $v = V/V_0$ , where  $V_0 = k_B T/(\eta\xi_0^2)$ . The final scaled system of equations is given as

$$\frac{d^2 v}{d\zeta^2} = \frac{v(\zeta)}{\cos \theta(\zeta)}, \quad (9)$$

$$\frac{d\theta}{d\zeta} = -g[\theta(\zeta)]v(\zeta), \quad (10)$$

where  $g[\theta] = [\cos \theta(2 - \cos^2 \theta)]^{3/2}/(6 - 7 \cos^2 \theta + 3 \cos^4 \theta)$ . These are subject to the following boundary conditions: (i)  $v = 0$  at  $\zeta = 0$  and (ii)  $dv/d\zeta = \dot{\gamma}\tau$  and  $\theta = 0$  at  $\zeta = h$ , where  $\tau = \eta\xi_0^3/k_B T$  is of order the characteristic hydrodynamic relaxation time of a blob of radius  $\xi_0$ . Equation (8) also yields the constraint condition

$$n_b \simeq \int_0^h d\zeta [2 - \cos^2 \theta(\zeta)]^{-1/3}, \quad (11)$$

where  $n_b = N(a/\xi_0)^{5/3}$  is the number of blobs in the unperturbed brush and  $h = H/\xi_0$ .

### III. RESULTS AND DISCUSSION

We have studied the solution of Eqs. (9)–(11) plus boundary conditions as a function of the dimensionless shear rate  $\dot{\gamma}\tau$  and the height of the unperturbed brush  $H_0 = n_b\xi_0$ . Figure 2 shows plots of the relative brush

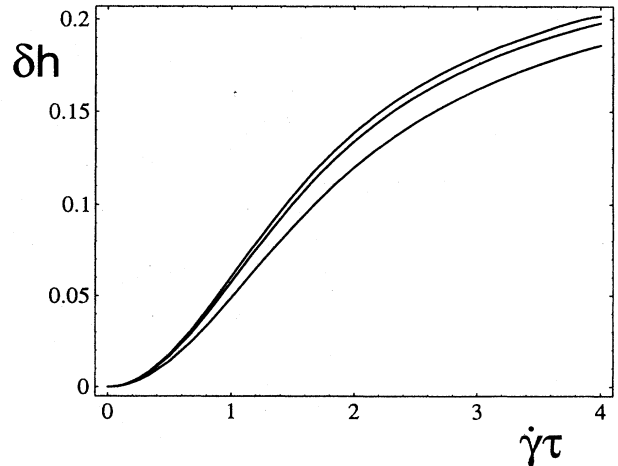


FIG. 2. Plots of the relative brush swelling  $\delta h = (H - H_0)/H_0$  vs  $\dot{\gamma}\tau$  for brushes initially with  $n_b = 5$  blobs (lowest curve),  $n_b = 10$  blobs (middle curve), and  $n_b = 15$  blobs (highest curve).

swelling  $\delta h = (H - H_0)/H_0$  vs  $\dot{\gamma}\tau$  for brushes initially with  $n_b = 5, 10,$  and  $15$  blobs. We find the onset of significant brush swelling at  $\dot{\gamma}\tau \simeq 1$ , followed by a saturation of swelling at large  $\dot{\gamma}\tau$ . Figure 3 shows the scaled solvent velocity profiles  $V/V_0$  vs  $z/H$  for the case of  $\dot{\gamma}\tau = 2$ , while Fig. 4 shows profiles of the associated tilt angle  $\theta$  and the scaled blob size  $\xi/\xi_0$ . These figures show that, roughly speaking, stretched chains can be divided into two regions: (i) an interior region of essentially uniform stretching and tilt in which  $V$  is very small and (ii) a boundary region of thickness  $\Delta z \simeq \xi_0$  of weakly stretched and tilted chains in which  $\xi(z)$  and  $\theta(z)$  vary rapidly. The thickness of this boundary layer corresponds roughly to the hydrodynamic penetration depth  $l_p \equiv [V(H)/V'(H)] \simeq \xi_0$  calculated from the velocity profiles (cf. Fig. 3).

Our results can be rationalized in terms of a “quasimonoblock” picture [25] in which uniformly tilted and stretched chains with constant blob size  $\xi_{MB}$  and tilt angle  $\theta_{MB}$  terminate in an unperturbed *virtual* end blob of size  $\xi_{end} \simeq \xi_0$ , as sketched in Fig. 5 [26]. If the drag force on this end blob  $f_{\parallel} \sim \eta V(H)\xi_0$ , obtained from the numerically computed velocity profile  $V(z)$ , is used to compute the uniform stretching of the remainder of the chain, the resulting  $\xi_{MB}$  and  $\theta_{MB}$  are in excellent accord with the numerically obtained  $\xi$  and  $\theta$  in the interior region. This picture explains both a qualitative similarity and a quantitative difference between our predictions and those of Barrat [13]. Barrat assumed a fixed blob size  $\xi_{MB}$  for all blobs including the outermost one. Under strong flows,  $\xi_{MB} \ll \xi_{end}$  and so this leads to an underestimate of  $f_{\parallel}$ . Moreover, it is clear from Fig. 2 that, for fixed grafting density and shear rate, short brushes swell less than longer ones. This can again be understood from the quasimonoblock picture: if brush swelling is analyzed on the basis of the stretching of the “active” interior portion of the grafted chains (disregarding the last blob of size  $\xi_{end}$ ), then the resulting  $\delta h$  is found to be almost independent of  $n_b$  (e.g.,  $\delta h \simeq 15\%$  for  $\dot{\gamma}\tau = 2$ ). Only in the limit

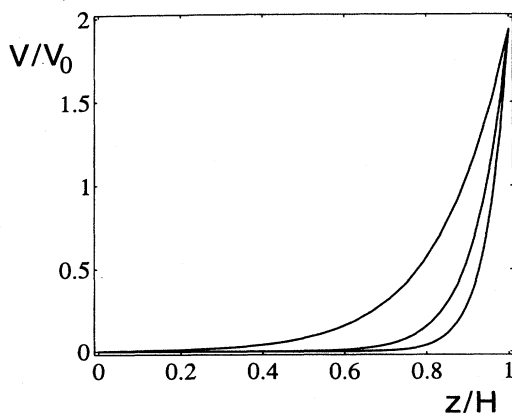


FIG. 3. Plots of the scaled solvent velocity profiles  $V/V_0$  as a function of the reduced distance  $z/H$  from the grafting surface for brushes initially with  $n_b = 5$  blobs (highest curve),  $n_b = 10$  blobs (middle curve), and  $n_b = 15$  blobs (lowest curve) sheared at  $\dot{\gamma}\tau = 2$ .

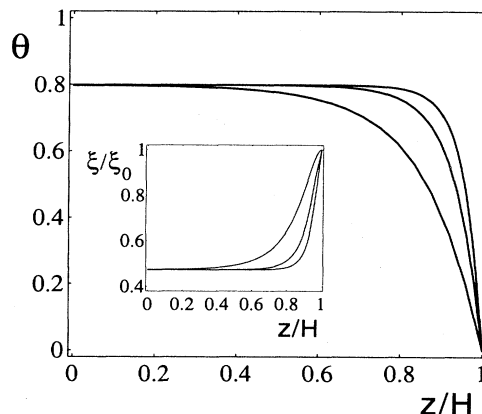


FIG. 4. Plots of the tilt angle  $\theta$  (in radians) and scaled blob size  $\xi/\xi_0$  vs  $z/H$  for  $\dot{\gamma}\tau = 2$ . The main plot shows  $\theta$  for brushes with  $n_b = 5$  blobs (lowest curve),  $n_b = 10$  blobs (middle curve), and  $n_b = 15$  blobs (highest curve), while the inset shows the analogous curves of  $\xi/\xi_0$  in reverse order.

of large  $n_b$  is this solvent penetration effect negligible (allowing the use of a pure monoblock approach, which ignores the details of solvent hydrodynamics [12,13]) and even then there are important consequences for  $f_{\parallel}$  as detailed above.

Our predictions should be directly relevant to neutron reflectivity experiments on brushes under shear [7–9], although it should be emphasized that quite high shear rates are required to achieve significant swelling [27]. Turning to the experiments of Ref. [3], we note that the solvent gap separating brush-bearing surfaces in relative motion decreases appreciably as the brushes swell. The solvent shear rate in the gap is accordingly not constant, but coupled to the brush swelling process. A detailed comparison of our model with these experiments thus requires a more elaborate analysis than we have given here. However, we may make some rough comparison with the steady-state conditions that prevail once the brushes have swollen into apparent contact at a critical velocity  $V_c$ . These have recently been interpreted in terms of a thin viscous lubrication layer of thickness  $d \sim \xi_0$  and effective viscosity  $\eta_{eff}$  separating the two

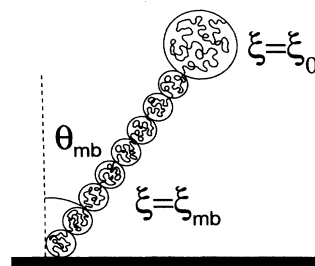


FIG. 5. Sketch of the “quasimonoblock” picture of an extended polymer chain as a section of uniformly tilted and stretched blobs with  $\xi = \xi_{MB}$  and  $\theta = \theta_{MB}$  in an essentially quiescent solvent, terminating in an unperturbed end blob of size  $\xi_{end} \simeq \xi_0$  in which the solvent velocity is nonvanishing.

sheared polymer brushes [5,6,28]. For the system studied in Ref. [3], one has  $V_c \simeq 0.0015 \text{ ms}^{-1}$ ,  $\xi_0 \simeq 100 \text{ \AA}$ , and  $\eta_{\text{eff}} \simeq 10^{-2} \text{ Pa s}$ , implying a characteristic relaxation time of  $\tau \simeq \eta_{\text{eff}} \xi_0^3 / k_B T \simeq 2.5 \mu\text{s}$ . Assuming linear shear flow in a lubrication film of thickness  $\xi_0$ , one has  $\dot{\gamma} \simeq V_c / \xi_0 \simeq 1.5 \times 10^5 \text{ s}^{-1}$ , giving  $\dot{\gamma} \tau \simeq 3/8$ . According to our model, this is roughly a factor of 10 smaller than that required to produce the experimentally reported brush swelling of  $\sim 20\%$ . This discrepancy is not surprising due to the uncertainties in the experimental parameters such as  $\eta_{\text{eff}}$  and in the various (unknown) numerical prefactors in our scaling theory and to various approximations, as detailed below.

The calculation we have described has inherent limitations. We have adopted the Alexander–de Gennes ansatz that all chains stretch alike. This approximation systematically underestimates the hydrodynamic penetration of solvent into the brush [11] and hence overestimates the crossover shear rate marking the onset of brush swelling. As mentioned previously, a fully self-consistent treatment would allow dispersion in the chain end positions. It would also require a more detailed description of hydrodynamic forces, perhaps along the lines of the multiple scattering theory of Ref. [29] for adsorbed homopolymer layers. This, however, would be a formidable numerical task. It seems likely that the decreasing density at the periphery of a real brush will have a strong effect on individual chain conformations, but it is less obvious that the global swelling behavior will be qualitatively affected. Work in progress, which allows for a partial relaxation of the Alexander–de Gennes ansatz, appears to support this

view [24]. The present approach is also limited by finite extensibility of the grafted polymer chains. For sufficiently high  $\dot{\gamma} \tau$ , the chains approach full extension and the blob concept employed in our model to estimate elastic and hydrodynamic forces breaks down. This regime, although experimentally relevant, would require a substantially modified theoretical analysis.

In conclusion, we have presented a mutually consistent theoretical approach addressing the deformation of grafted polymer layers in strong (solvent) shear flows. Our calculations for polymer brushes in shear flows compare well with earlier, *ad hoc* methods in suitable limits. This helps establish the validity of our theoretical approach, which provides a solid starting point for more refined treatments of grafted polymer layers in strong flows. Furthermore, our approach may be readily extended to address more general problems involving interfacial polymer layers in strong shear flows. Work in progress is considering the details of chain deformation and desorption in grafted polymer layers [24] and in adsorbed polymer layers [30] in strong shear flows, the latter complementing recent studies in the linear regime [29,31].

#### ACKNOWLEDGMENTS

We thank M. Aubouy, T. Cosgrove, J. Klein, M. Rafailovich, J. Sokolov, and C. Toprakcioglu for interesting discussions and correspondence. This work was supported in part by the EPSRC and the DTI Colloid Technology Programme.

- 
- [1] S.T. Milner, *Science* **251**, 905 (1991).
  - [2] A. Halperin, M. Tirrell, and T.P. Lodge, *Adv. Polym. Sci.* **100**, 33 (1992).
  - [3] J. Klein, D. Perahia, and S. Warburg, *Nature* **352**, 143 (1991).
  - [4] J. Klein, Y. Kamiyama, H. Yoshizawa, J.N. Israelachvili, G.H. Fredrickson, P. Pincus, and L.J. Fetters, *Macromolecules* **26**, 5552 (1993).
  - [5] J. Klein, *Colloids Surf. A* **86**, 63 (1994).
  - [6] J. Klein, E. Kumacheva, D. Perahia, D. Mahalu, and S. Warburg, *Faraday Discuss.* **98**, 173 (1994).
  - [7] M. Rafailovich and J. Sokolov (private communication).
  - [8] C. Toprakcioglu (private communication).
  - [9] T. Cosgrove (private communication).
  - [10] G.H. Fredrickson and P. Pincus, *Langmuir* **7**, 786 (1991).
  - [11] S.T. Milner, *Macromolecules* **24**, 3704 (1991).
  - [12] Y. Rabin and S. Alexander, *Europhys. Lett.* **13**, 49 (1990).
  - [13] J.-L. Barrat, *Macromolecules* **25**, 832 (1992).
  - [14] V. Kumaran, *Macromolecules* **26**, 2464 (1993).
  - [15] S. Alexander, *J. Phys. (Paris)* **38**, 983 (1977).
  - [16] P.G. de Gennes, *J. Phys. (Paris)* **37**, 1443 (1976); *Macromolecules* **13**, 1069 (1980).
  - [17] S.T. Milner, T.A. Witten, and M.E. Cates, *Europhys. Lett.* **5**, 413 (1988); *Macromolecules* **21**, 2610 (1988).
  - [18] A.M. Skvortsov, A.A. Gorbunov, I.V. Pavlushkov, E.B. Zhulina, O.V. Borisov, and V.A. Priamitsyn, *Vysokomol. Soedin. A* **30**, 1615 (1988); E.B. Zhulina, V.A. Priamitsyn, and O.V. Borisov, *ibid.* **31**, 185 (1989).
  - [19] P. Pincus, *Macromolecules* **9**, 386 (1976).
  - [20] A. Ajdari, F. Brochard-Wyart, P.G. de Gennes, L. Leibler, J.-L. Viovy, and M. Rubinstein, *Physica A* **204**, 17 (1994); M. Rubinstein, A. Ajdari, L. Leibler, F. Brochard-Wyart, and P.G. de Gennes, *C. R. Acad. Sci. Paris II* **316**, 317 (1993).
  - [21] F. Brochard-Wyart, *Europhys. Lett.* **23**, 105 (1993).
  - [22] F. Brochard-Wyart, H. Hervet, and P. Pincus, *Europhys. Lett.* **26**, 511 (1994).
  - [23] J.L. Harden and M.E. Cates, *J. Phys. (France) II* **5**, 1093 (1995); **5** 1757 (1995).
  - [24] M. Aubouy, J.L. Harden, and M.E. Cates (unpublished).
  - [25] See Refs. [12,13] for a description of the usual monoblock approach to brushes.
  - [26] The boundary conditions on our continuum equations imply  $\xi = \xi_0$  at the extremity of the brush. Strictly, however, the continuum limit breaks down at this point and

- $\xi_{\text{end}}$  should be obtained from the solution of  $\xi_{\text{end}} = \xi(z = H - \xi_{\text{end}})$ , which is somewhat less than  $\xi_0$ . However, since solvent flow penetrates to a depth  $\xi_0$ , the effective drag force  $f_{\parallel}$  is actually determined by  $\xi_0$  rather than  $\xi_{\text{end}}$ .
- [27] For  $\xi_0 = 1000 \text{ \AA}$ , corresponding to a very modest grafting density, and for a typical solvent viscosity of  $10^{-3} \text{ Pa s}$ , the onset of significant swelling occurs at  $\dot{\gamma} \simeq 4000 \text{ s}^{-1}$ .
- [28] J. Klein (private communication).
- [29] D.T. Wu and M.E. Cates, *Phys. Rev. Lett.* **71**, 4142 (1993).
- [30] J.L. Harden, M. Aubouy, and M.E. Cates (unpublished).
- [31] P. Sens, C.M. Marques, and J.-F. Joanny, *Macromolecules* **27**, 3812 (1994).